Proceedings of the XVIII ECSMGE 2024
GEOTECHNICAL ENGINEERING CHALLENGES
TO MEET CURRENT AND EMERGING NEEDS OF SOCIETY

ISBN 978-1-032-54816-6
DOI 10.1201/9781003431749-289

Calibration of a numerical model for the investigation of piled rafts under dynamic loading

Étalonnage d'un modèle numérique pour l'étude des radeaux de pieux sous chargement dynamique

Y. Degu*
Department of Geotechnical Engineering, University of Kassel, Kassel, Germany and Faculty of Civil; Water Resources Engineering, Bahir Dar University, Bahir Dar, Ethiopia

O. Reul
Department of Geotechnical Engineering, University of Kassel, Kassel, Germany

A. Worku
School of Civil and Environmental Engineering, Addis Ababa University, Addis Ababa, Ethiopia

F. Tschuchnigg
Institute of Soil Mechanics, Foundation Engineering and Computational Geotechnics, Graz University of Technology, Graz, Austria

**yideg@uni-kassel.de*

ABSTRACT: Limited knowledge available on the soil-structure interaction of piled rafts under cyclic and dynamic loading together with gaps in national building codes frequently prevents the design of technically and economically optimised foundations for sensitive structures, such as foundations for high-rise buildings or bridges. As the first step in a research project to investigate the bearing behaviour of piled rafts under dynamic loading, existing model tests and in-situ measurements are evaluated to provide a database for the calibration of numerical models. This paper focuses on the numerical back-analysis of the centrifuge model tests on piled rafts by Horikoshi et al. (2003a; 2003b). The 3D finite element model employs the Hardening Soil model with small-strain stiffness (HSsmall) to simulate the material behaviour of the Toyoura sand used in the model tests. In the scope of this work, the calibration process of the material parameters and the results of the back-analysis of the model tests are presented.

RÉSUMÉ: Les connaissances limitées disponibles sur l'interaction sol-structure des radeaux de pieux sous charge cyclique et dynamique, ainsi que les lacunes des codes de construction nationaux, empêchent souvent la conception de fondations techniquement et économiquement optimisées pour les structures sensibles, telles que les fondations des immeubles de grande hauteur ou des ponts. Dans le cadre de la première étape d'un projet de recherche visant à étudier le comportement des radeaux de pieux sous charge dynamique, les essais sur modèle et les mesures in situ existants sont évalués afin de fournir une base de données pour l'étalonnage des modèles numériques. Cet article se concentre sur la rétro-analyse numérique des essais en centrifugeuse effectués sur des radeaux de pieux par Horikoshi et al. (2003a ; 2003b). Le modèle d'éléments finis 3D utilise le sol durcissant avec une rigidité à faible déformation (HSsmall) pour simuler le comportement du matériau du sable de Toyoura utilisé dans les essais sur modèle. Dans le cadre de ce travail, le processus d'étalonnage des paramètres matériels et les résultats de la rétro-analyse des essais sur modèle sont présentés.

Keywords: Piled raft; dynamic loading; centrifuge test; numerical analysis; HSsmall soil model.

1 INTRODUCTION

The piled raft is a well established foundation system especially for tall buildings (e.g. O'Neill et al, 1996, Poulos, 2001, Reul and Randolph, 2003) under predominantly vertical static loading. For this load case a guideline for design, dimensioning and construction already exists (ISSMGE Technical Committee 212, 2013) with piled rafts designed according to this guideline termed Combined Pile-Raft Foundations (CPRF). Also, piled rafts are applied frequently for bridge foundations (e.g. Hecht and Dürrwang, 2001, Comodromos et al., 2016) where lateral loads generally are of more importance. However, in contrast to piled rafts under predominantly vertical loading, comparatively few in-situ measurements on completed structures and large-scale model tests (field investigations) have been documented for piled rafts under combined vertical and horizontal loading, regardless of whether monotonic, cyclic or dynamic actions are involved. To investigate the bearing behaviour of piled rafts under complex loading conditions small scale model tests as well as centrifuge model tests have been carried out by different researchers (e.g. Horikoshi et al., 2003a; 2003b; Sawada and Takemura, 2014; Unsever et al., 2014; Hamada et al., 2015).

In some recent studies, the behaviour of piled rafts under dynamic loading conditions was studied numerically using model tests as a means of validation (e.g. Eslami et al., 2011; Kumar et al., 2016; Bhaduri and Choudhury, 2019; Akbari et al., 2021). However, frequently the capability to realistically capture main aspects of soil-structure-interaction is limited by the use of linear elastic-perfectly plastic soil models, which generate only elastic strains upon small strain load reversals. Evidently, more advanced constitutive models are vital to model for example hysteretic damping.

The current research projects aims on providing a better understanding of the bearing behaviour of piled rafts under lateral monotonic and dynamic loading by means of numerical simulations with the finite element method (FEM) applying the Hardening Soil model with small-strain stiffness. This paper presents the results of the first phase of the project with the calibration of the material parameters of HSsmall model for dry Toyoura sand by means of the back-analysis of the centrifuge model tests employing of 3D finite element analysis (FEA).

2 CALIBRATION OF THE HSSMALL MODEL

The HSsmall model (Benz, 2007) is an extension of the standard Hardening Soil (HS) model (Schanz et al., 1999) incorporating two additional parameters: the shear modulus at a very small strain G_0^{ref} and the threshold shear strain $\gamma_{0.7}$, the shear strain at which the secant shear modulus G_s^{ref} is degraded to $0.72 \cdot G_0^{ref}$. Thus, the model accounts for the small strain stiffness, which can be related to a degrading secant stiffness with an S-shaped characteristics curve according to the formulation of Santos and Correia (2001) and an accompanying increasing damping ratio with increasing strain amplitudes. As a result, it reproduces hysteretic elastic soil behaviour in loading-reloading cycles leading to hysteretic damping.

Most of the model parameters of the HSsmall model for Toyoura sand were calibrated using the tool Plaxis SoilTest for simulating element tests where the hypoplastic parameters for Toyoura sand provided by Herle and Gudehus (1999) and Ng et al. (2013) were used as a reference.

Due to the limited space available, in the following, the description of the calibration procedure is restricted to the two parameters mainly controlling the material behaviour at small strains, namely G_0^{ref} and $\gamma_{0.7}$. The reference small strain shear stiffness modulus G_0^{ref} was estimated by means of three different approaches which all yielded similar values. In the first approach, an initial tangent slope of a hysteretic loop of a cyclic triaxial test simulation was evaluated. Alternatively, G_0^{ref} was determined by making use of the secant shear stiffness at a very small shear strain, where the secant shear stiffness in turn was determined from the deviatoric stress and shear strain values of standard triaxial test simulation. In the third approach, the initial Young's modulus E_0^{ref} of the standard triaxial test was used to determine the small strain shear stiffness from

$$G_0^{ref} = E_0^{ref} / \left(2 \cdot (1 + \nu_{ur})\right) \tag{1}$$

where $\nu_{ur} = 0.2$ was employed as suggested by Benz (2007). Additionally, the obtained result was compared with the values extracted from charts by Alpan (1970) and Benz (2007), showing reasonable agreement.

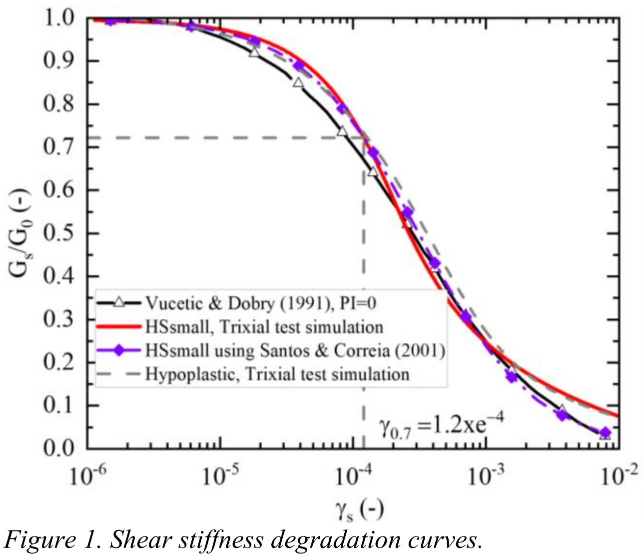

Figure 1. Shear stiffness degradation curves.

The second small strain parameter, the threshold shear strain $\gamma_{0.7}$, was calibrated using an iterative curve fitting procedure with reference to the secant shear modulus degradation and damping ratio curves of the reference hypoplastic model. The degradation curves were generated from deviatoric stress and small strain values of the triaxial simulation results and using the approach by Santos and Correia (2001). The result was further refined by fitting with the secant shear modulus reduction curves of Vucetic and Dobry (1991) for a zero plasticity index value. As shown in Figure 1, the shear stiffness degradation curves of the current study are in good agreement with the hypoplastic reference model result and the curve presented by Vucetic and Dobry (1991).

The basic parameters defining the HSsmall model and their calibrated values, as determined from the calibration process, are listed in Table 1. It has to be noted that a cohesion was introduced for the reason of increasing numerical stability (in the dynamic FEA). This approach appears to be legitimate since the focus of the research project is on the serviceability rather than the ultimate capacity of foundations.

Table 1. Calibrated HSsmall model parameters.

Parameters		Description	Values
E_{50}^{ref}	MPa	reference secant stiffness at 50% of q_f	42.1
E_{oed}^{ref}	MPa	Tangent oedometric stiffness	30.2
E_{ur}^{ref}	MPa	unloading-reloading stiffness	126.9
ν_{ur}	-	unloading-reloading Poisson's ratio	0.2
m	-	power for stress-level dependency of stiffness	0.65
p^{ref}	kPa	reference stress for stiffness	100.0
G_0^{ref}	MPa	reference shear stiffness at very small strain	149.0
$\gamma_{0.7}$	-	threshold shear strain at which $G_s = 0.722 \cdot G_0$	$1.20 \cdot 10^{-4}$
c	kPa	cohesion	5.8
φ	°	angle of internal friction	35.6
ψ	°	angle of dilatancy	8.7
K_0^{nc}	-	at rest earth pressure coefficient for NC soil	0.47
R_f	-	failure ratio (q_f/q_a)	0.9

3 NUMERICAL MODEL

The numerical simulation of the centrifuge tests by Horikoshi et al. (2003a; 2003b) was carried out with the program PLAXIS 3D in prototype scale applying the appropriate scaling laws (e.g. Muir Wood, 2004). The dimensions of piles and raft as well as the material properties applied in the 3D FEA are summarised in Table 2. The piles were installed "wished-in-place" in the FE model which is considered to capture the installation process in the centrifuge tests reasonably well where the sand was poured around the piles at 1g level.

The soil as well as the piles and the raft were modelled with 10-node tetrahedral volume elements. Between soil and piles, respectively between soil and raft 12-node interface elements, with $R_{int} = 0.59$, are located. The piles and the raft are rigidly connected. The finite element mesh is shown in Figure 2 together with the boundary conditions applied at the lateral and bottom surfaces of the model for both static and dynamic loading conditions, reflecting the situation in the centrifuge model tests. For dynamic loading conditions, energy dissipation is reproduced by introducing free field boundary conditions at the side boundaries in the direction of loading and by using Rayleigh damping in addition to the hysteretic damping considered in the chosen constitutive model.

In FEA, careful selection of the mesh size plays a vital role in ensuring the accuracy of the numerical analysis at an optimum computational time. Accordingly, the size of the model and the discretisation were systematically varied to check and minimise their effect on the analysis. Based on convergence of the results and computing time criteria, a fine-sized mesh with additional refinement in the vicinity of the foundation was generated. For dynamic loading, the mesh size should be smaller than one-eighth of the wavelength associated with the maximum frequency component of the input motion, as suggested by Kuhlemeyer and Lysmer (1973). A typical model comprising 82698 elements and 131867 nodes with an average element size of 0.68 m fulfills this criteria.

Table 2. Model dimensions and additional parameters.

Parameter		Loading types	
		Vertical (Static)	Horizontal (Static/ Dyn*)
Pile (Solid)			
Length	m	8.5	9.0
Diameter	m	0.5	0.5
Unit weight	kN/m³	9.72	9.72
Young's modulus	GPa	41.7	41.7
Raft			
Thickness	m	1.25	2.00
Width	m	4	4
Unit weight	kN/m³	27	27
Young's modulus	GPa	71	71
Soil			
Width	m	20	20
Length	m	35	35
Depth	m	23.5	23.0/16.0*
Unit weight	kN/m³	15.2	15.2
Initial void ratio	-	0.75	0.75
Interface			
Interface str., R_{int}	-	0.59	0.59

* dynamic loading

The loads were applied similar to the procedure followed in the centrifuge test. For the monotonic loading conditions, the loads were employed in two stages. In the first stage, the vertical load was applied as a raft weight plus an additional vertical pressure. Whereas in the subsequent stage, the monotonic loads were applied by means of prescribed displacement cycles in their respective directions. Similarly, for the dynamic loading case, the vertical load was induced by making use of an increased unit weight of the raft, and the horizontal dynamic load was excited at the bottom of the soil model by applying harmonic loading of 1 m/s^2 amplitude and frequency of 1 Hz for 20 s with an additional 5 s steady- state (zero amplitude) condition before and after the main excitation. For both the static and dynamic lateral loading cases, a total vertical load of 5751 kN was applied, equalling a total mass of 4.69 kg in the model scale. Moreover, Rayleigh damping was introduced by employing damping coefficients $\alpha = 0.52$, and $\beta = 0.0027$, at a damping ratio of 5%.

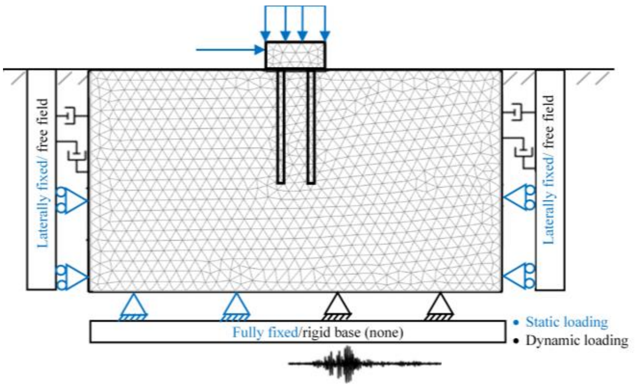

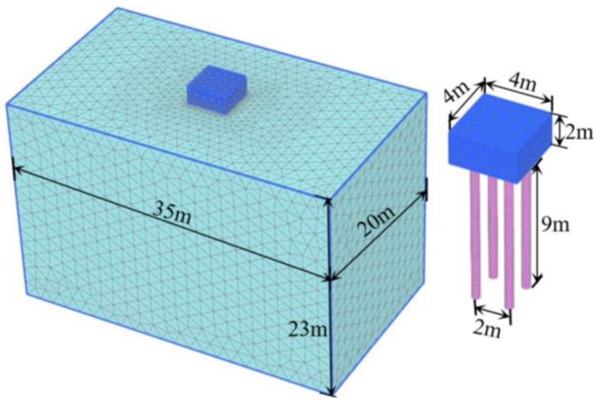

Figure 2. Schematic illustration and FE mesh of the model for static lateral loading case.

4 COMPARISON OF CENTRIFUGE TESTS AND NUMERICAL SIMULATIONS

4.1 Static vertical and horizontal loading

To validate the numerical model and verify the suitability of the selected constitutive model and its model parameters the results of 3D FEA are compared to the respective centrifuge test results on piled rafts. The results for the vertical monotonic load test are presented in Figure 3 and Figure 4 showing a very good agreement between centrifuge model tests and numerical simulation.

The minor difference in the vertical load share is probably related to software limitations in extraction of the structural forces of the piles. The vertical settlement is also compared with numerical analysis result provided by Alnuaim et al. (2017) using a linear elastic-perfectly plastic soil model with a Mohr Coulomb's failure criteria.

The variation of the horizontal displacement and the horizontal stiffness, defined by the ratio of the horizontal load to the horizontal displacement, is compared and presented in Figure 5 and Figure 6, respectively.

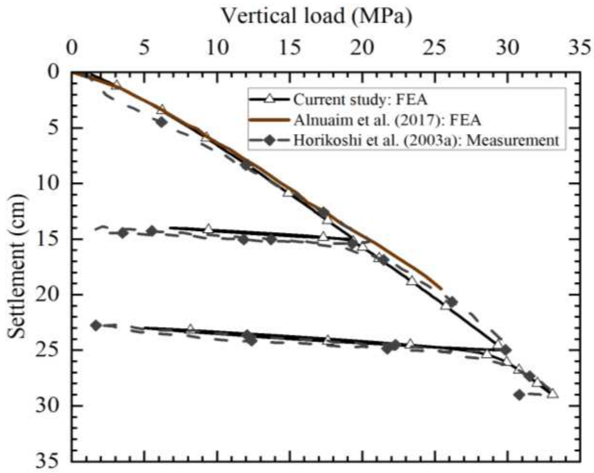

Figure 3. Vertical loading: Variation of settlement with load.

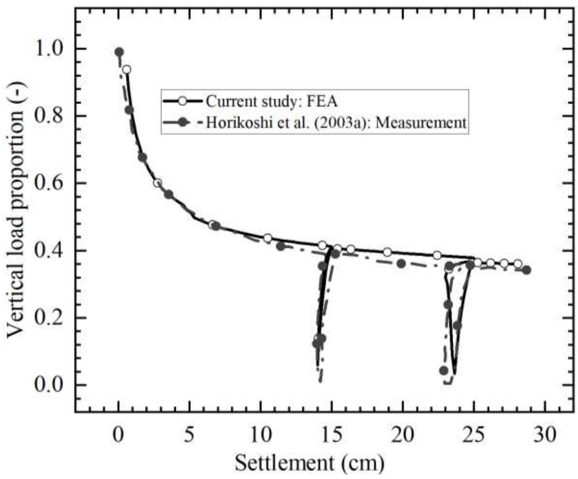

Figure 4. Vertical loading: Variation of pile load share with settlement.

4.2 Dynamic horizontal loading

Back analyses conducted for dynamic loading conditions also revealed a reasonable agreement with the test results. For example, the measured and simulated acceleration and settlement time histories at the top of the raft are compared in Figure 7 and Figure 8, respectively. The maximum acceleration response at the top of the raft was also compared with the numerical results of Eslami et al. (2011) and Kumar et al. (2016), where a linear elastic-perfectly plastic soil model was used. The comparison indicates that the results achieved with the HSsmall model is in better agreement with the measurements than the two models justifying the application of this more advanced model, particularly for dynamic loading cases.

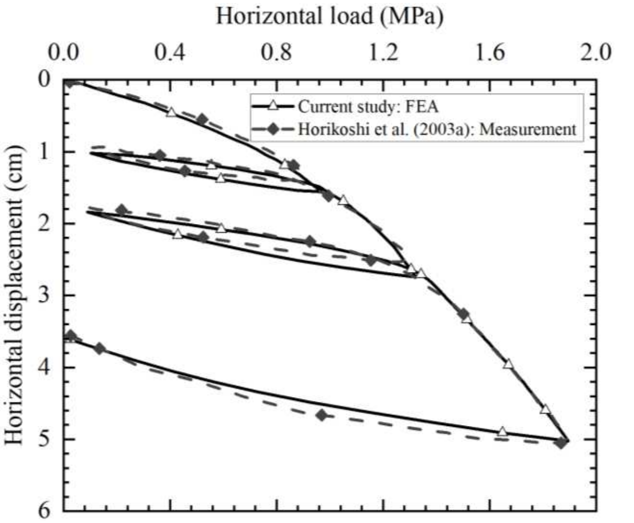

Figure 5. Horizontal loading: Variation of horizontal displacement with load.

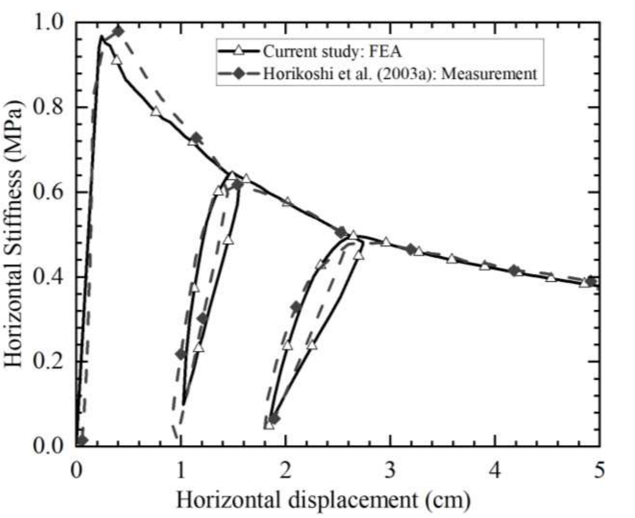

Figure 6. Horizontal loading: Variation of horizontal stiffness with horizontal displacement.

5 CONCLUSIONS

In this work, the calibration of the parameters of the HSsmall model and the validation of 3D numerical model by means of back-analysing centrifuge model tests on piled rafts in sand were presented. Most of the calibrated material parameters were derived by more than one method obtaining similar results. From the validation process, it can be concluded that the 3D numerical model in combination with the HSsmall constitutive model are reasonably well suited for the analysis of piled rafts under static as well as dynamic conditions.

In the next step of the research project the calibrated and verified numerical model will be used for an extensive study investigating piled rafts subjected to different loading conditions.

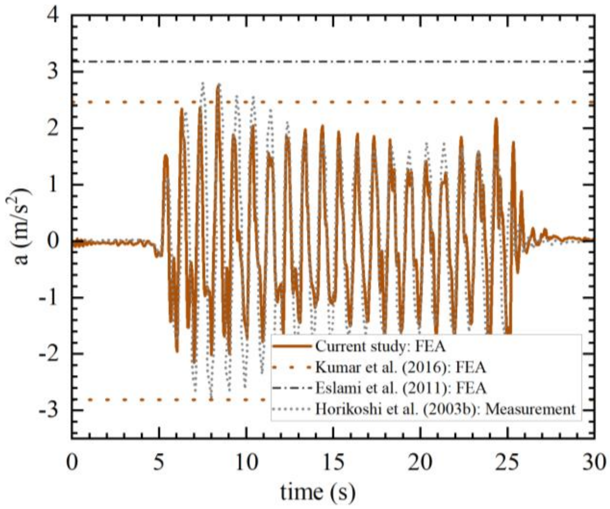

Figure 7. Dynamic loading: Comparison of variation of acceleration at the top of the raft with time.

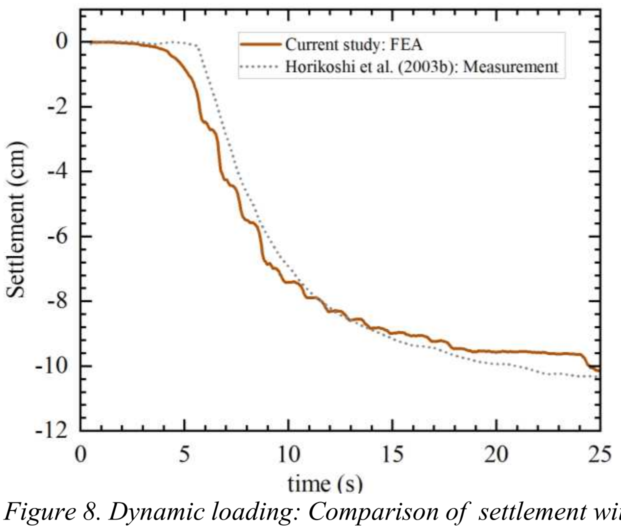

Figure 8. Dynamic loading: Comparison of settlement with time from FEA and test result.

ACKNOWLEDGMENTS

This work is financially supported by Bahir Dar University, the Catholic Academic Exchange Service, the Ethiopian Ministry of Education, the German Academic Exchange Service, and the University of Kassel. The authors are grateful for the financial support.

REFERENCES

Akbari, A., Eslami, A. and Nikookar, M. (2021). Influence of soil stiffness on the response of piled raft foundations under earthquake loading, *Transp. Infrastruct. Geotech.* 8(4), pp. 590–606. https://doi.org/10.1007/s40515-021-00157-8.

Alnuaim, A. M., El Naggar, H. and El Naggar, M. H. (2017). Evaluation of piled raft performance using a verified 3D nonlinear numerical model, *Geotech. Geol. Eng.* 35(4), pp. 1831–1845. https://doi.org/10.1007/s10706-017-0212-1.

Alpan, I. (1970). The geotechnical properties of soils, *Earth-Science Reviews* 6(1), pp. 5–49. https://doi.org/10.1016/0012-8252(70)90001-2.

Benz, T. (2007). *Small-strain stiffness of soils and its numerical consequences,* PhD thesis, Universität Stuttgart, Institut für Geotechnik, Stuttgart.

Bhaduri, A. and Choudhury, D. (2019). Influence of connection rigidity on combined pile-raft foundation under seismic loading. In *Earthquake Geotech. Eng. for Protection and Development of Envir. and Const.,* Rome, Italy, pp. 1437–1444.

Brinkgreve, R., Bonnier, P. and Kappert, M. (2007). Hysteretic damping in a small-strain stiffness model, X, Pande, G. N., Pietruszczak, S. (Eds.). In *Numerical Models in Geomechanics,* Rhodes, Greece, pp. 737–742. https://doi.org/10.1201/NOE0415440271.ch106.

Comodromos, E. M., Papadopoulou, M. C. and Laloui, L. (2016). Contribution to the design methodologies of piled raft foundations under combined loadings, *Can. Geotech. J.* 53(4), pp. 559–577. https://doi.org/10.1139/cgj-2015-0251.

Eslami, M. M., Aminikhah, A. and Ahmadi, M. M. (2011). A comparative study on pile group and piled raft foundations (PRF) behavior under seismic loading, *Comp. Meth. Civil Eng.,* 2(2), pp. 185–199.

Hamada, J., Tsuchiya, T., Tanikawa, T. and Yamashita, K. (2015). Lateral loading tests on piled rafts and simplified method to evaluate sectional forces of piles, *Geotech. Eng. J. of the SEAGS and AGSSEA,* 46(2), pp. 29–42.

Hecht, T. and Dürrwang, R. (2001). Optimierung der Gründung der Reichenbachtalbrüke mit der Kominierten Pfahl-Plattengrüdung, In *Pfahl-Symposium*, Braunschweig, Germany, 65, pp. 21–34. (in German).

Herle, I. and Gudehus, G. (1999). Determination of parameters of a hypoplastic constitutive model from properties of grain assemblies, *Mech. Cohes.-Frict. Mater.* 4(5), pp. 461–486. https://doi.org/10.1002/(SICI)1099-1484(199909)4:5<461::AIDCFM71>3.0.CO;2-P.

Horikoshi, K., Matsumoto, T., Hashizume, Y., Watanabe, T. and Fukuyama, H. (2003a). Performance of piled raft foundations subjected to static horizontal loads, *Int. J. of Physical Modelling in Geotech.* 3(2), pp. 37–50. https://doi.org/10.1680/ijpmg.2003.030204.

Horikoshi, K., Matsumoto, T., Hashizume, Y. and Watanabe, T. (2003b). Performance of piled raft foundations subjected to dynamic loading, *Int. J. of Physical Modelling in Geotech.* 3(2), pp. 51–62. https://doi.org/10.1680/ijpmg.2003.030205.

ISSMGE Technical Committee 212 (2013). ISSMGE combined pile-raft foundation guideline, Katzenbach, R. and Choudhury, D. (Eds.), Darmstadt, Germany.

Kuhlemeyer, R. L. and Lysmer, J. (1973). Finite element method accuracy for wave propagation problems, *J. Soil Mech. and Found. Div.* 99(5), pp. 421–427. https://doi.org/10.1061/JSFEAQ.0001885.

Kumar, A., Choudhury, D. and Katzenbach, R. (2016). Effect of earthquake on combined pile–raft foundation, *Int. J. Geomech.* 16(5), pp. 04016013: 1–16. https://doi.org/10.1061/(ASCE)GM.1943-5622.0000637.

Muir Wood, D. (2004). *Geotechnical Modelling*. 1st ed., CRC Press, London. https://doi.org/10.1201/9781315273556.

Ng, C. W., Shi, J. and Hong, Y. (2013). Three-dimensional centrifuge modelling of basement excavation effects on an existing tunnel in dry sand, *Can. Geotech. J.* 50(8), pp. 874–888. https://doi.org/10.1139/cgj-2012-0423.

O'Neill, M. W., Caputo, V., De Cock, F., Hartikainen, J. and Mets, M. (1996). Case histories of pile-supported rafts (Report for ISSMFE-Technical Committee TCl8, University of Houston, Texas).

Poulos, H. G. (2001). Piled raft foundations: design and applications, *Géotechnique* 51(2), pp. 95–113. https://doi.org/10.1680/geot.51.2.95.40292.

Reul, O. and Randolph, M. F. (2003). Piled rafts in overconsolidated clay: comparison of in situ measurements and numerical analyses, *Géotechnique* 53(3), pp. 301–315. https://doi.org/10.1680/geot.2003.53.3.301.

Santos, J. A. and Correia, A. G. (2001). Reference threshold shear strain of soil. Its application to obtain an unique strain-dependent shear modulus curve for soil. In *15th Int. Conf. on Soil Mech. and Geotech. Eng.,* Istanbul, Turkey. Vol. 1, pp. 267–270.

Sawada, K. and Takemura, J. (2014). Centrifuge model tests on piled raft foundation in sand subjected to lateral and moment loads, *Soils and Foundations* 54(2), pp. 126–140. https://doi.org/10.1016/j.sandf.2014.02.005.

Schanz, T., Vermeer, P. A. and Bonnier, P. G. (1999). The hardening soil model: formulation and verification. In *Beyond 2000 in Computational Geotechnics*, Ronald B.J. Brinkgreve (Ed.), pp. 281–296. https://doi.org/10.1201/9781315138206-27.

Unsever, Y. S., Matsumoto, T., Shimono, S. and Ozkan, M. Y. (2014). Static cyclic load tests on model foundations in dry sand, *Geotech. Eng. J. of the SEAGS & AGSSEA,* 45(2), pp. 40–51

Vucetic, M. and Dobry, R. (1991). Effect of soil plasticity on cyclic response, *J. of Geotech. Eng.*117(1), pp. 89–107. https://doi.org/10.1061/(ASCE)0733-9410(1991)117:1(89).